SMiRT-12 / K. Kussmaul (Editor)

INFLUENCE OF MANUFACTURING PROCESS ON THE IN-REACTOR CREEP ANISOTROPY OF STRESS RELIEVED ZIRCALOY-2 CLADDING

S.H. Shann and L.F. Van Swam

Siemens Power Corporation, P.O. Box 130, Richland, WA 99352, USA

ABSTRACT

A procedure to determine the axial/radial and circumferential/ radial contractile strain ratios (the R and P factors in the Backofen modified von Mises-Hill yield criterion) from post-irradiation dimensional measurements of Zircaloy-2 cladding of BWR fuel rods, tie rods, and water rods was developed and has been described during the previous SMiRT Conference[Shann and van Swam]. The present study employs the procedure to determine the anisotropy factors R and P for textured cold-worked stress-relieved (CWSR) Zircaloy-2 cladding fabricated by different manufacturing processes. The analysis indicates that the cladding manufacturing process has a pronounced effect on the anisotropy of irradiation induced creep. Cladding types with identical yield and ultimate tensile strength but fabricated by different manufacturing processes have different values of R and P during in-reactor creep.

1.0 INTRODUCTION

A procedure was developed and has previously been published (SMiRT-11 Conference) for the determination of the contractile strain ratios (R and P factors) for irradiation induced creep[Shann and van Swam]. This procedure used deformation measurements on irradiated BWR assemblies and fuel rods to calculate the R and P values for stress-relieved Zircaloy-2 cladding during irradiation.

Improved corrosion behavior of Zircaloy-2 in BWRs has been obtained by Siemens Power Corporation (SPC) through alteration of the heat treatment of Zircaloy-2 cladding and other changes in the tubing fabrication processes. The altered manufacturing processes affected the corrosion resistance and also the creep and growth behavior. This paper describes work performed to determine the contractile strain ratios R and P of four alternative cladding types during in-reactor creep.

2.0 MODEL DESCRIPTION

The model published in the SMiRT-11 Conference[Shann and van Swam] has been used for the analyses. The model uses the creep correlation for textured anisotropic zircaloy expressed by the following equations[Murty and Adams]:

$$\sigma_g^2 = \frac{R(\sigma_r-\sigma_\theta)^2 + RP(\sigma_\theta - \sigma_z)^2 + P(\sigma_z-\sigma_r)^2}{P(R+1)} \tag{1}$$

$$\begin{bmatrix}\dot{\epsilon}_r\\ \dot{\epsilon}_\theta\\ \dot{\epsilon}_z\end{bmatrix} = \frac{\dot{\epsilon}_g}{P(R+1)\sigma_g} \cdot \begin{bmatrix}(R+P) & -R & -P\\ -R & R(P+1) & -RP\\ -P & -RP & P(R+1)\end{bmatrix}\begin{bmatrix}\sigma_r\\ \sigma_\theta\\ \sigma_z\end{bmatrix} \tag{2}$$

where
σ_r, σ_θ, & σ_z = radial, circumferential, & axial stress
ϵ_r, ϵ_θ, & ϵ_z = stress-induced radial, circumferential, & axial strain
σ_g and ϵ_g = generalized stress and strain
R and P = axial/radial and circumferential/radial contractile strain ratios.

Before the onset of pellet-cladding interaction and using the Gittus stress dependence:

$$\epsilon \propto \sigma^{1.23} \tag{3}$$

The following correlation can then be derived for rods with a stress ratio of x ($x = \sigma_\theta/\sigma_z$) :

$$\epsilon_z \propto \frac{\epsilon_g}{\sigma_g}\left(\frac{1-(x-1)R}{X(R+1)}\right)\sigma_\theta \tag{4}$$

The generalized stress in the tie rods can be calculated from Equation (1) assuming that $\sigma_r = 0$:

$$\sigma_g = \left[\frac{PR+R-\frac{2}{x}PR+\frac{PR}{x^2}+\frac{P}{x^2}}{P(R+1)}\sigma_\theta^2\right]^{1/2} \tag{5}$$

With the assumption that the standard fuel rods and the tie rods in a fuel assembly experience similar hoop stress early in life, it follows that :

$$\frac{\epsilon_z \text{ tie rod}}{\epsilon_z \text{ fuel rod}} = \left[\frac{PR+R-\frac{2}{x}PR+\frac{PR}{x^2}+\frac{P}{x^2}}{R+\frac{PR}{4}+\frac{P}{4}}\right]^{0.115}\frac{1-(x-1)R}{1-R}\frac{2}{x} \tag{6}$$

With irradiation induced growth determined from water rod growth data and solving Equations (4), (5), and (6) with fuel rod diametral creepdown and growth as well as tie rod growth measurement data, the R and P values for irradiation induced creep of textured Zircaloy-2 tubing can be determined.

3.0 CLADDING TYPES STUDIED

Figure 1 graphically represents the manufacturing process for the different cladding types. Cladding types A, B and C are made by the same process, the only difference being the intermediate annealing temperature employed in the rocking (size reduction) annealing sequence. The manufacturing of these cladding types is indicated in the left side branch of Figure 1. Type B cladding used a 50°C lower intermediate annealing temperature than type A, and type C used a 100°C lower temperature. The fabrication process of the LBQ (late beta-quenched) cladding is indicated in the right side branch of Figure 1. An additional beta-quench process is performed later in the manufacturing process.

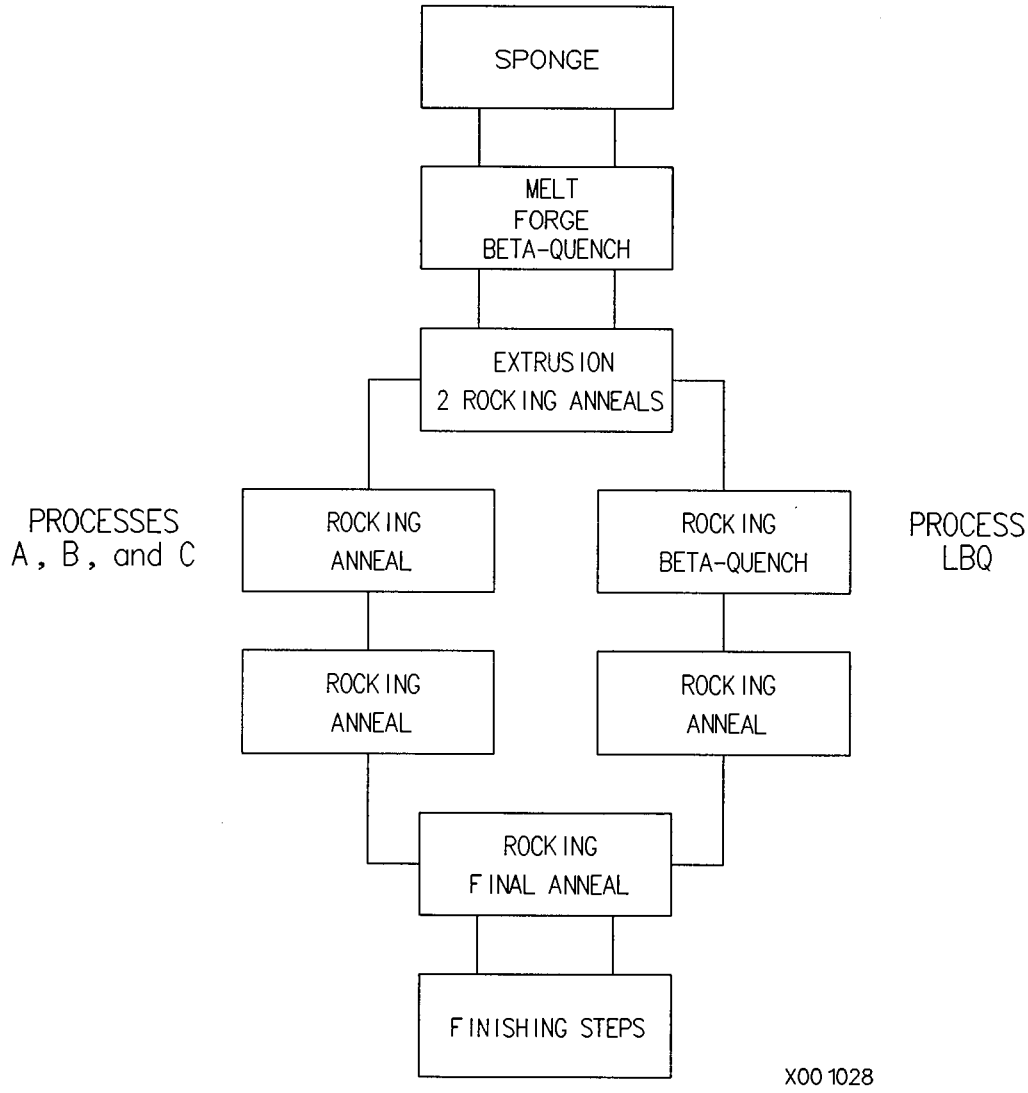

Figure 1 Fabrication Processes for Various Cladding Types

All cladding types were manufactured to the same yield and ultimate tensile strength. The contractile strain ratios R and P were calculated from the post-irradiation measured fuel rod, tie rod, and water rod deformation measurements.

4.0 DATA BASE USED IN CONTRACTILE STRAIN RATIO DETERMINATION

Rod growth data and rod creepdown data on fuel from a number of BWRs were used to obtain the R and P values for the cladding types studied. Tables 1 through 4 summarize the number of data analyzed for cladding types A, B, C, and LBQ, respectively. The cladding type A data were obtained from measurements in 5 BWRs, type B data in 6 BWRs, type C data in 5 BWRs, and type LBQ data in 4 BWRs.

The axial deformation data consists of a single measured value per rod; multiple diametral deformation data were obtained along the rod at various axial locations.

The SMiRT-11 paper considered data from cladding type A only. As shown in Table 1, the data base on type A cladding has been expanded for the current analysis.

Table 1. Data base used in analysis of cladding type A

	# of data	# of rods measured	# of assemblies measured
Fuel Rod Diametral Deformation Data	1377	219	14
Fuel Rod Axial Deformation Data	219	219	14
Water Rod Axial Deformation Data	13	13	7
Tie Rod Axial Deformation Data	28	28	7

Table 2. Data base used in analysis of cladding type B

	# of data	# of rods measured	# of assemblies measured
Fuel Rod Diametral Deformation Data	189	32	6
Fuel Rod Axial Deformation Data	66	66	9
Water Rod Axial Deformation Data	2	2	1
Tie Rod Axial Deformation Data	-	-	-

Table 3. Data base used in analysis of cladding type C

	# of data	# of rods measured	# of assemblies measured
Fuel Rod Diametral Deformation Data	140	25	4
Fuel Rod Axial Deformation Data	56	56	7
Water Rod Axial Deformation Data	-	-	-
Tie Rod Axial Deformation Data	-	-	-

Table 4. Data base used in analysis of cladding type LBQ

	# of data	# of rods measured	# of assemblies measured
Fuel Rod Diametral Deformation Data	527	86	7
Fuel Rod Axial Deformation Data	161	161	6
Water Rod Axial Deformation Data	2	2	2
Tie Rod Axial Deformation Data	16	16	2

5.0 RESULTS AND DISCUSSION

5.1 Results of data analysis

The measured fuel rod growth data for the different cladding types were first statistically analyzed by using a Student's t-test to confirm that the data for the different types were statistically distinguishable from one another. The t-test indicated that the probability for LBQ and for cladding type A, B and C rod growth data to be two different populations was larger than 95%.

Figure 2 graphically compares the fuel rod growth of cladding types A, B, and C. Growth data for assemblies which contain rods with cladding types A, B, and C side-by-side are plotted. Each data point in this figure is an assembly averaged value of fuel rod growth data for all rods with one cladding type in a given assembly. The line in the figure is the regression fit of all currently available cladding type A rod growth data. The comparison indicates that cladding types A, B and C had very similar rod growth and the differences in growth of these three cladding types are not statistically significant.

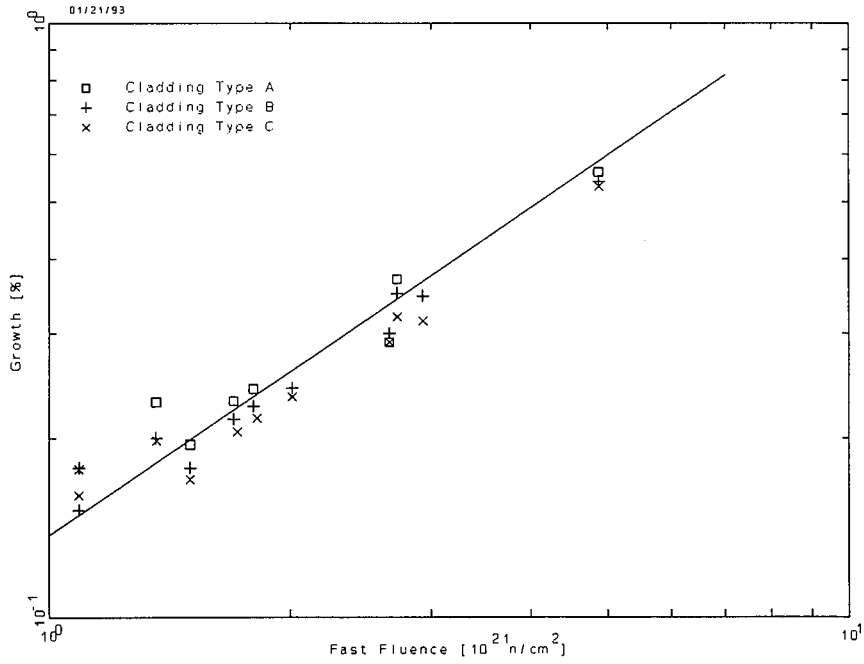

Figure 2 Comparison Of Fuel Rod Growth Data For Cladding Types A, B, And C

Figure 3 compares the water rod growth for cladding type B with that for cladding type A. The water rod growth data for cladding type B are limited. The available data in Figure 3 indicates that stress-free irradiation-induced growth is identical for cladding types A and B.

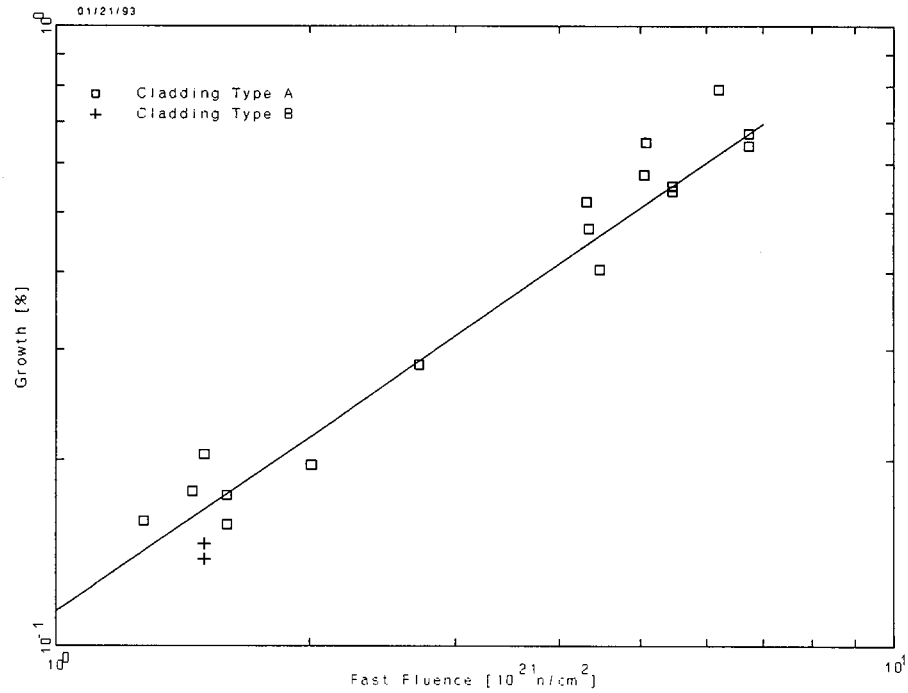

Figure 3 Comparison Of Water Rod Growth Data For Cladding Types A, B, And C

5.2 Determination of R and P values for irradiated Zircaloy-2

Analysis of the expanded data base of type A cladding yielded the same results as before, the R and P values were 1.38 and 2.39, respectively, for type A cladding.

Types B and C cladding had the same post-irradiation diametral and axial deformation as type A cladding. Calculations with the R and P values determined for type A cladding gave a good fit to the measured data of cladding types B and C. Figures 4 and 5 show the results. The two figures provide the measured and the calculated assembly-averaged cladding creep and cladding growth, respectively. Figures 4 and 5 indicate that cladding types B and C have the same contractile strain ratios for in-reactor creep as cladding type A.

The axial stress in the tie rods resulting from the holddown spring force on the fuel rods was calculated for assemblies with LBQ cladding. The hoop to axial stress ratio in the tie rods for the assemblies measured ranged from 2.52 to 2.76. Use of the analysis outlined in Section 2 yielded values for R and P for LBQ cladding of 2.51 and 1.98, respectively.

The combined effects of creep anisotropy and irradiation induced growth give LBQ cladding similar diametral creep as type A, B and C cladding but make LBQ cladding grow less than cladding types A, B and C.

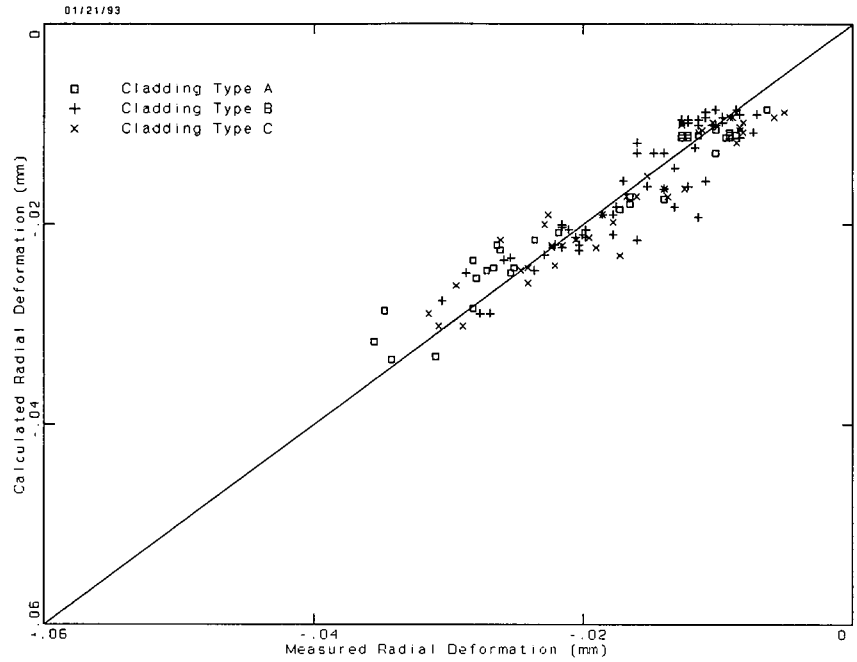

Figure 4 Creep Predictions For Cladding Types A, B, And C

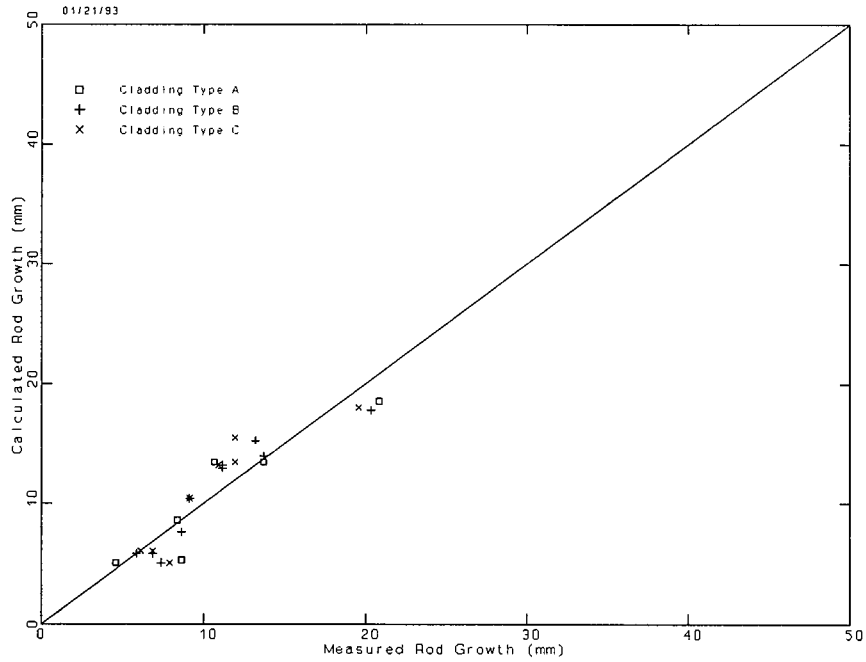

Figure 5 Fuel Rod Growth Predictions For Cladding Types A, B, And C

5.3 Comparison with measured results in unirradiated Zircaloy-2

Tensile tests were performed on unirradiated Zircaloy-2 tubing at 382°C and an R value was determined from these tests. Table 5 lists the results. The test results indicate that LBQ cladding had a different contractile strain ratio R compared to the other three cladding types. The results for in-reactor creep and growth behavior (Section 5.2) are included for comparison. As shown in this table, both the R determined from tensile tests on unirradiated cladding at 382°C and R for in-reactor creep and growth are higher for LBQ cladding than for the other cladding types. However, the R factor derived from tensile testing at elevated temperature can not be used for predictions of in-reactor creep and growth behavior of Zircaloy-2 cladding.

Table 5 Comparison of Tensile Test and In-Pile Creep R Values

Cladding Type	382°C Tensile Test Results		Irradiation Induced Creep
	Average	Standard Deviation	
A, B, & C	1.29	0.32	1.38
LBQ	1.91	0.35	2.51

6.0 SUMMARY

The R and P contractile strain ratios for irradiation induced creep of four types of stress-relieved Zircaloy-2 cladding were calculated. The four cladding types were fabricated using different manufacturing processes to impart improved corrosion resistance to Zircaloy-2 cladding. The cladding received a final anneal that provided similar yield and ultimate tensile strength to all the cladding types.

In-reactor creep and growth measurements indicate that the contractile strain ratios (R and P) for Zircaloy-2 are manufacturing process dependent. Three cladding types with similar manufacturing processes but slightly different intermediate annealing temperatures had similar R and P values (1.38 and 2.39, respectively). LBQ cladding with a different manufacturing process had a different set of R and P values (2.51 and 1.98, respectively).

The R and P ratios calculated from the post-irradiation deformation data were compared with those determined from tensile tests of un-irradiated cladding. The comparison indicates that tensile tests at elevated temperature and irradiation-induced creep are governed by different contractile strain ratios. However, the trend in R value is the same: LBQ cladding has a higher R value for irradiation induced creep and a 382°C tensile test in comparison with the equivalent R values for the three other cladding types.

REFERENCES

Murty,K.L. and Adams,B.L., 1985, Biaxial Creep of Textured Zircaloy I: Experimental and Phenomenological Descriptions, Mat. Sci. and Eng., 70 169.

Gittus,J.H., Howl,D.A. and Hughes,H., 1970, Theoretical Analysis of Cladding Stress and Strains Produced by Expansion of Cracked Fuel Pellets, Nucl. Appl. and Technol., 9 40.

Shann,S.H. and van Swam,L.F., 1981, Creep Anisotropy of Zircaloy-2 Cladding during Irradiation, Transaction of the 11th International Conference on Structure Mechanics in Reactor Technology, Vol. C.